

## Improvement of Light-Harvesting Efficiency of TiO<sub>2</sub> Granules Through Chemical Interconnection of Nanoparticles by Adding TEOT to Spray Solution

Mi Ja Lim\*, Shin Ae Song\*\*, Yun Chan Kang\*\*\*, Won-Wook So\*\*\*\* and Kyeong Youl Jung\*,†

\*Department of Chemical Engineering, Kongju National University, 1223-24 Cheonan-Daero, Seobuk-gu, Cheonan 31080, Korea

\*\*Micro Manufacturing System Technology Center, Korea Institute of Industrial Technology,  
143 Hanggaul-ro, Sangnok-gu, Ansan-si, Gyeonggi 15588, Korea

\*\*\*Department of Materials Science and Engineering, Korea University, 145 Anam-ro, Seongbuk-gu, Seoul 02841, Korea

\*\*\*\*Energy Materials Research Center, Korea Research Institute of Chemical Technology, Sinseongno 19, P.O.Box 107, Daejeon 34106, Korea  
(Received 13 March 2015; Received in revised form 30 March 2015; accepted 27 March 2015)

**Abstract:** Mesoporous TiO<sub>2</sub> granules were prepared by spray pyrolysis using nano-sized titania particles which were synthesized by a hydrothermal method, and they were evaluated as the photoanode of dye-sensitized solar cells. To enhance the cell efficiency, nanoparticles within granules were chemically interconnected by adding titanium ethoxide (TEOT) to colloidal spray solution. The resulting titania particles had anatase phase without forming rutile. TiO<sub>2</sub> granules obtained showed about 400 nm in size, the specific surface area of 74-77 m<sup>2</sup>/g, and average pore size of 13-17 nm. The chemical modification of TiO<sub>2</sub> granules by adding TEOT initially to the colloidal spray solution was proved to be an effective way in terms of increasing both the light scattering within photoanode and the lifetimes of photo-excited electrons. Consequently, the light-harvesting efficiency of TEOT-modified granules ( $\eta=6.72\%$ ) was enhanced about 14% higher than primitive nanoparticles.

Key words: Titania Granules, Chemical Modification, DSSC, Spray Pyrolysis, Electron Lifetimes

### 1. Introduction

Dye-sensitized solar cells (DSSCs) are considered excellent photovoltaic devices which can convert the solar energy into the electricity because they have simple structure, low production cost and large flexibility of colors and shapes [1-4]. Since the first demonstration of dye-sensitized solar cells by Grätzel and co-workers in 1991, there have been many efforts to improve the solar-to-electric power-conversion efficiency (PCE) of DSSCs. As a result, the PCE of DSSCs has reached 12%, through the development of high efficient photoanodes [5-7], dyes [8] and electrolytes [9].

Among the components of DSSCs, the performance of DSSCs strongly depends on the properties of photoanodes. In general, photoanodes are constructed by casting a dye-sensitized mesoporous semiconductor film on a transparent conductive substrate. To achieve high power conversion efficiency, photoanodes should be well designed to have as high as possible a surface area, electron diffusion rate and light scattering [10]. In particular, the transport of photo-excited electrons through a porous photoanode layer is a key factor determining the cell performance. Thus, many researchers have given large efforts to designing the nanostructure of photoan-

odes in order to enhance the electron transport within the photoanode layer with minimizing the recombination reaction. For achieving high performance of DSSCs, photoelectrons after being excited by the light absorption of dye molecules should be successfully injected first to the conduction band of TiO<sub>2</sub>, and thereafter they are needed to be efficiently extracted from porous photoanodes toward transparent conducting films. To efficiently extract electrons out to the photoanode, TiO<sub>2</sub> nanoparticles should be connected well to each other within porous electrodes. A typical porous photoanode, constructed by using TiO<sub>2</sub> nanocrystalline, has a long and complicated path for electron diffusion because the connections between TiO<sub>2</sub> nanoparticles are poor. Consequently, the loss of electrons in the conduction band of TiO<sub>2</sub> takes place inevitably through recombination processes at the interface of TiO<sub>2</sub> nanoparticles before escaping the photoanode. To overcome this issue, titania nanorods or nanotubes have been studied. The diffusion rate of photo-excited electrons toward TCO electrodes was reported to be improved by making titania nanotubes, vertically aligned on the transparent conducting electrode (TCO) [11,12]. Nevertheless, the reported photo-conversion efficiency of rod-type TiO<sub>2</sub> is lower than the traditional nanoparticle-based TiO<sub>2</sub> film because of the low surface area of nanorods.

Typically, nano-sized TiO<sub>2</sub> thin films are transparent and have poor light scattering characteristics, which hampers the performance of DSSCs. Thus, the use of a light-scattering layer is an effective way to enhance the cell efficiency. Recently, submicron-sized titania beads with mesopores were reported to be better than nanoparticles in

†To whom correspondence should be addressed.

E-mail: kyjung@kongju.ac.kr

‡This article is dedicated to Prof. Kyun Young Park on the occasion of his retirement from Kongju National University.

This is an Open-Access article distributed under the terms of the Creative Commons Attribution Non-Commercial License (<http://creativecommons.org/licenses/by-nc/3.0>) which permits unrestricted non-commercial use, distribution, and reproduction in any medium, provided the original work is properly cited.

both electron lifetime and light scattering, which make it possible to reach the cell efficiency over 10% without using any light scattering layers [13]. In addition, the use of submicron-sized TiO<sub>2</sub> beads generates voids, helping for the electrolyte to permeate well into the porous photoanode. TiCl<sub>4</sub> treatment is also known as an effective way to improve the cell efficiency because it results in the increase of electron lifetimes as the result of better connections between nanoparticles in photoanodes [14–16]. Given these results reported previously, the direct formation of chemical interconnection between nanoparticles at the preparation step of granules is expected to be beneficial for improving the efficiency of DSSCs. To prove this, in this work, we prepared mesoporous titania granules having a diameter of about 400–450 nm by a spray pyrolysis process using the colloidal solution containing nano-sized TiO<sub>2</sub>. To have proper chemical connectivity between nanoparticles in the granules, in this work, titanium ethoxide (TEOT) was initially added to the colloidal spray solution as a chemical-connecting agent. As a result, the in-situ formation of a proper anatase layers between the nanoparticles could be achieved during the preparation of TiO<sub>2</sub> granules. The chemical connection effect on the light-harvesting efficiency of DSSCs was investigated by the measurements of X-ray diffraction (XRD), UV/visible reflectance, photovoltaic properties and electrochemical impedance spectroscopy (EIS).

## 2. Experimental

### 2-1. Synthesis of TiO<sub>2</sub> granules

TiO<sub>2</sub> granules were prepared from nano-sized TiO<sub>2</sub> colloidal solution by an ultrasonic spray pyrolysis process that consists of an ultrasonic aerosol generator with 17 vibrators of 1.7 MHz, a quartz tube (inner diameter = 55 mm, length = 1000 mm), and a Teflon bag filter. Nano-sized TiO<sub>2</sub> colloidal solution was prepared by a typical hydrothermal method at 180 °C. To generate the chemical interconnection of nanoparticles in granules, titanium ethoxide (TEOT, Aldrich) was dissolved in purified water of 250 mL containing HNO<sub>3</sub> of 10 mL, and followed by mixing with the colloidal solution. Herein, the molar percentage of TEOT with respect to the total Ti precursor was fixed at 20%. The prepared spray colloidal solutions were atomized by an ultrasonic aerosol generator (1.7 MHz) to produce many droplets, and carried by air (30 liter/min) into the quartz reactor at 900 °C. The resulting granule powder was collected by a bag filter, and used for the fabrication of photoelectrodes without any treatment.

### 2-2. Fabrication of DSSC using the granulized particles

Titania paste was prepared by mixing nano-sized particles or sub-micron-sized granules (0.5 g) with terpinol (solvent, 1.5 g) and ethyl cellulose (binder, 0.2 g). The mixture of titania, binder and solvent was mixed homogeneously by using a centrifugal mixer (THINKY Co. ARM-310) for 30 min and a three-roll milling process. Working electrode having the active area of 0.35 cm<sup>2</sup> was prepared by the following procedure. First, a dense and thin blocking layer on FTO

glass (1.4 cm × 0.8 cm) was formed by using TiCl<sub>4</sub> aqueous solution (0.04 M). For this, after the TiCl<sub>4</sub> solution was dropped on the FTO substrate, it was dried in a convection oven for 20 min at 70 °C. Thereafter, the resulting dense film (TiO<sub>2</sub> blocking layer) was washed by ethanol. Next, a porous TiO<sub>2</sub> layer on the TiCl<sub>4</sub>-treated dense film was formed by a doctor-blade method using the electrode paste prepared in advance, and followed by the heat treatment for 10 min at 550 °C.

Dye adsorption was achieved by immersing porous TiO<sub>2</sub> films in ethanol solution containing N719 dye (0.25 mM) for 18 h at room temperature under excluding the outside light. Counter electrode films were also prepared by the doctor-blade method using a Pt paste on the FTO glass. Two holes were drilled before forming the Pt film. The prepared Pt paste film was calcined at 400 °C (10 °C/min) for 20 min. Next, the dye-impregnated TiO<sub>2</sub> working electrodes with the Pt-counter electrodes were assembled as a sandwich type cell by melting Surlyn sealant (DuPont, 60 μm thickness) on a hot plate at 180 °C. Electrolyte (EL-HSE, DYESOL) was injected into the inside of cells through the holes made at the Pt-counter electrode. Finally, the holes were sealed by melting a Surlyn film using a soldering iron. A conceptual diagram explaining the electrode structure is shown in Fig. 1. The sample name of the photoanode fabricated by using nanoparticles themselves was given as S1 (case I in Fig. 1). The photoanode comprising granule particles prepared from the spray solution without the TEOT precursor were denoted as S2 (case II in Fig. 1), and the granules prepared from the TEOT-added spray solution were denoted as S3 (case III in Fig. 1).

### 2-3. Characterization

The microstructure and morphological properties of prepared nanoparticles and granules were measured by scanning electron microscopy (SEM, TESCAN, MIRA LHM) and transmission electron microscopy (TEM, JEOL, JEM1210). The specific surface area, pore size, and pore volume of prepared granules were obtained from the nitrogen adsorption-desorption isotherms measured by Micromeritics ASAP 2020. The change of crystallographic form was monitored by X-ray diffraction (XRD, RIGAGU RINT-2100) measurement. The diffused light scattering characteristics of the photoanodes before the

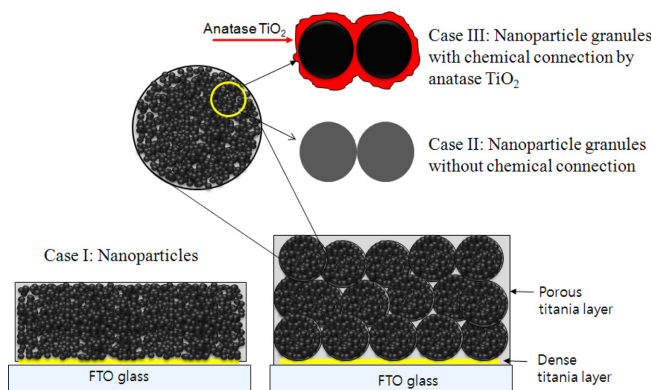


Fig. 1. Concept diagram showing the difference of photoanodes.

dye loading were monitored by UV-vis spectrophotometer (Shimadzu, UV-2450).

Photovoltaic performance of DSSCs was evaluated by measuring the current-voltage (J-V) characteristic curves using a solar simulator (McScience, K101 LAB20). The simulated light power was calibrated to one sun ( $100 \text{ mW/cm}^2$ ) using a reference Si photodiode. Electrochemical impedance spectroscopy measurements (AutoLAB, PGSTAT30) under the illumination of light (1 sun) were performed at the open circuit voltage ( $V_{oc}$ ) bias with the frequency range from 0.01 Hz to 100 kHz.

### 3. Results and Discussion

#### 3-1. Physical properties of granulized particles

Fig. 2(a) and (b) are TEM and SEM images of pristine nanoparticles and granules prepared by the spray pyrolysis, respectively. Fig. 2(c) and (d) are the particle size distributions and  $\text{N}_2$  adsorption/desorption isotherms of granular particles. Hydrothermally synthesized  $\text{TiO}_2$  has a particle size of about 20–25 nm. The granules show a spherical shape, having a monodisperse size distribution between 300 nm and 600 nm. The particle size distribution of granular particles was not affected by the use of TEOT. The  $\text{N}_2$  adsorption/desorption isotherms of  $\text{TiO}_2$  granules have a typical type IV with hysteresis curves which are typically observed in mesoporous materials. Pore size distributions are displayed as the inset of Fig. 2(d). The isotherm data indicate that titania granules have well-developed mesopores. Texture properties for nano-sized primitive particles and submicron-sized granular particles are summarized in Table 1. There is no big decrease in the BET surface area by the TEOT addition to the colloidal spray solution. However, the addition of TEOT causes the increment of

**Table 1. Summary of pore properties, photovoltaic characteristics, charge transfer resistance, and electron lifetime of DSSCs based on different photoanodes**

Sample name	S1	S2	S3
type	Nanoparticles	Granules	Granules
$S_{BET}$ , $\text{m}^2/\text{g}$	68	77	74
Pore volume, $\text{cm}^3/\text{g}$	-	0.29	0.35
Average pore size, nm	-	13.1	16.5
Average particle size, nm	20–25	400	403
$V_{oc}$ , V	0.83	0.84	0.83
$J_{sc}$ , $\text{mA/cm}^2$	9.8	9.3	11.1
FF	0.73	0.72	0.73
PCE ( $\eta$ ), %	5.89	5.60	6.72
$R_2$ , $\Omega$	6.7	8.2	5.6
Electron lifetime ( $\tau_e$ ), ms	8.6	6.3	11.7

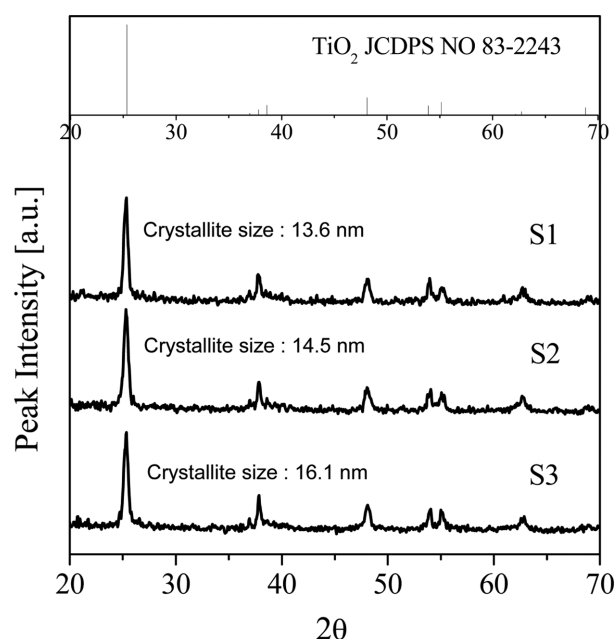


**Fig. 3. XRD patterns of  $\text{TiO}_2$  particles.**

pore size and pore volume, and this result indicates that the primary particle size of granules is enlarged by forming chemical interconnection between nanoparticles as shown in the case III of Fig. 1.

To identify the crystallographic changes, the XRD patterns for  $\text{TiO}_2$  nanoparticles (S1) and granules (S2 and S3) prepared by the spray pyrolysis are shown in Fig. 3. All samples show pure anatase phase, and no rutile phase was observed. The crystallite size was calculated by Scherrer equation and shown in Fig. 3. The calculated crystallite sizes are 13.6 nm (S1), 14.5 nm (S2) and 16.1 nm (S3). The crystallite sizes of granules are larger than that of primitive nanoparticles, which indicates that the grain growth of nanoparticles occurs during the granulation at  $900^\circ\text{C}$ . Furthermore, the sample S3, prepared from the colloidal solution containing TEOT, has a crystallite size larger than that of the sample S2. Given this, it was concluded that the added TEOT took part in an additional grain growth of granules by interconnecting primary nanoparticles.

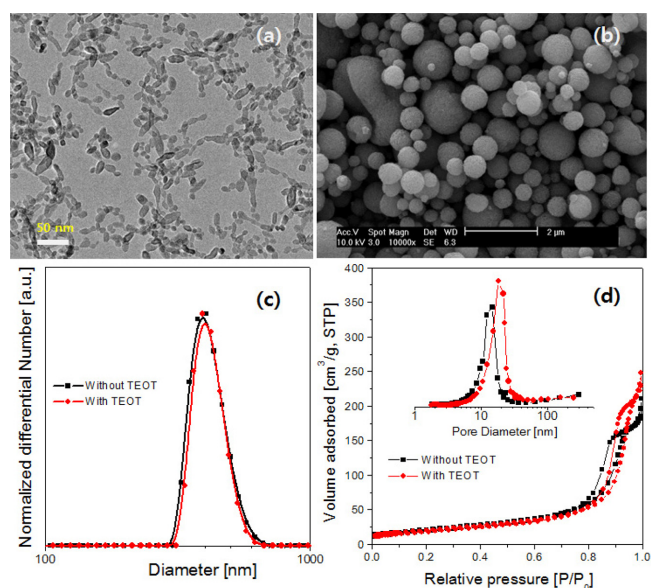


**Fig. 2. (a) TEM and SEM images for nanoparticles and granulized particles, respectively. Particle size distribution (c) and  $\text{N}_2$  adsorption/desorption isotherm (d) of granulized particles.**

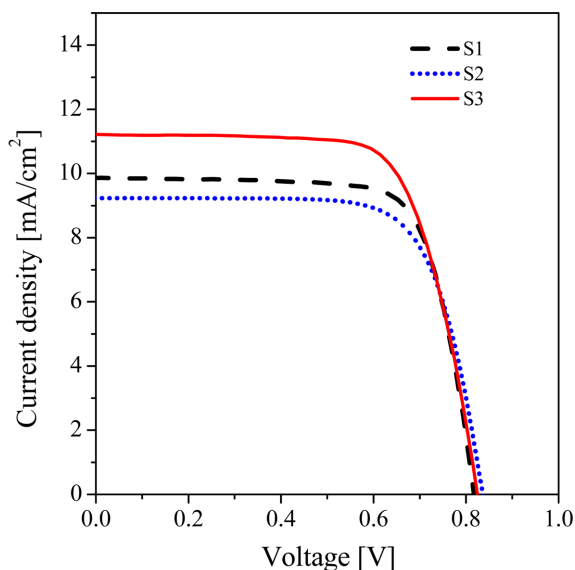


Fig. 4. I-V curves of photoanodes fabricated by using nanoparticles (S1) and granules (S2 and S3).

### 3-2. Photovoltaic, light scattering, and impedance characterization of DSSCs

To evaluate the performance as a working electrode for DSSC, three different photoanode films were fabricated by using titania samples (nanoparticles and granules). The current density-voltage ( $J$ - $V$ ) curves obtained under simulated 1.5 AM solar illumination are shown in Fig. 4. Detailed photovoltaic characteristics are summarized in Table 1. The cell efficiency of the granules (S2) prepared without the TEOT addition is lower than that of the nanoparticles. However, the TEOT-added granules (S3) have a cell efficiency higher than the nanoparticles (S1). The three electrodes show no significant difference in the open-circuit voltage ( $V_{oc}$ ) and the fill factor ( $FF$ ), but there is a big difference in the current density ( $J_{sc}$ ). The electrode S3 (granules prepared with TEOT) had the largest current density. That is, by the chemical connection of nanoparticles in granules, the current density was increased from 9.27 (S2) to 11.1 mA/cm<sup>2</sup> (S3). As a result, the cell efficiency of the S3 electrode ( $\eta = 6.72\%$ ) was improved about 20% compared with that of the S2 electrode ( $\eta = 5.60\%$ ).

The light-scattering ability of TiO<sub>2</sub> electrodes is important in enhancing the light-harvesting efficiency. To check the light-scattering behavior, the diffuse reflectance of photoanodes prepared before the dye loading was measured, and the results are shown in Fig. 5. The films composed of mesoporous granules showed an improved diffuse reflectance compared with that of the nanoparticle film. That is, the granulized TiO<sub>2</sub> films are better than the nanoparticle film in the scattering of incident light, especially in the wavelength range longer than 450 nm [17]. Moreover, the TEOT-added granules (S3) showed an improved reflectance in the whole region of visible light. Therefore, we concluded that the enhancement of the diffuse reflectance via the chemical connection of nanoparticles within granules contributed to increasing the light-harvesting efficiency of the S3 electrode.

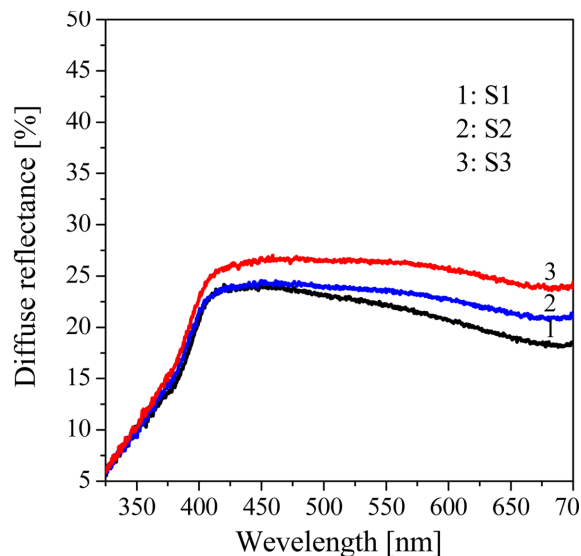


Fig. 5. UV-vis diffuse reflectance of the photoanodes before the dye loading.

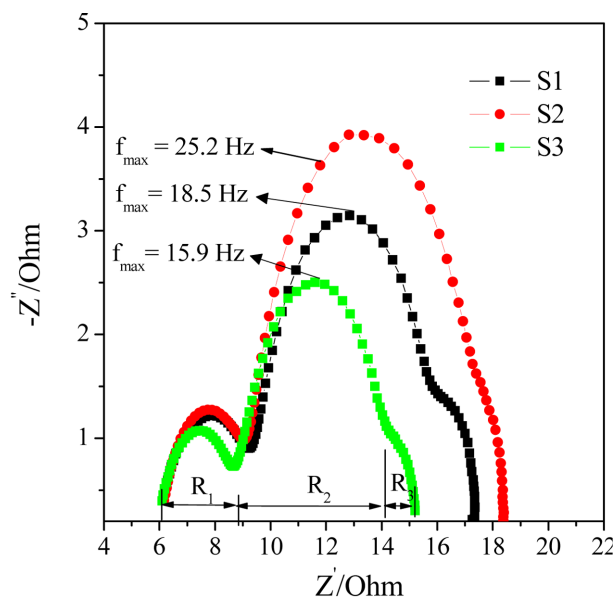


Fig. 6. Nyquist plot of EIS data for the DSSCs having three different photoanodes.

Electrochemical impedance spectroscopy (EIS) measurements were conducted to investigate the charge transfer processes in the prepared photoanodes. Fig. 6 shows Nyquist plots of the EIS data obtained at the applied bias of  $V_{oc}$  in the frequency range from 0.1 Hz to 100 kHz. Typically, Nyquist plots for the impedance of dye-sensitized solar cells consist of three semicircle arcs. The first small semicircle in the high-frequency region is attributed to the charge-transfer process ( $R_1$ ) at the counter electrode, the largest semicircle at the intermediate-frequency region corresponds to impedance related to the charge-transfer processes ( $R_2$ ) in the TiO<sub>2</sub>/dye/electrolyte interface, and the third semicircle in the low-frequency region is related to the resistance ( $R_3$ ) for the Nernstian diffusion of electrolyte [18]. The charge transfer resistance ( $R_2$ ) was estimated from the circle width

in the intermediate-frequency region, and the resulting values are summarized in Table 1. The  $R_2$  value (8.2  $\Omega$ ) for granular  $\text{TiO}_2$  ( $S_2$ ) prepared without TEOT is larger than that (6.7  $\Omega$ ) of the electrode ( $S_1$ ) fabricated using nano-sized  $\text{TiO}_2$  itself. This result means that the interconnectivity of nanoparticles within granules is poor when they are prepared without adding TEOT. On the other hand, the  $R_2$  value (5.6  $\Omega$ ) of the electrode  $S_3$  is smaller than those of other two photoanodes. Also, the  $R_3$  value of granular  $\text{TiO}_2$  (1.1  $\Omega$  and 0.88  $\Omega$  for the  $S_2$  and  $S_3$  electrodes, respectively) is smaller than that of nano-sized  $\text{TiO}_2$  (1.42  $\Omega$ ). This indicates that more efficient diffusion of  $\text{I}_3^-$  ions occurs in the electrodes having granular  $\text{TiO}_2$ . Given this, the chemical modification of granules by adding TEOT in the granulation process proves to be an effective way to reduce the resistance in the  $\text{TiO}_2$ /dye/electrolyte interface as well as the diffusion resistance of the electrolyte.

The electron lifetime ( $\tau_e$ ) can be estimated by the relation  $\tau_e = 1/(2\pi f_{\max})$ , where  $f_{\max}$  is the peak frequency of the semicircle observed in the middle-frequency region of the EIS data [19]. The peak frequency,  $f_{\max}$  is given in Fig. 6. The calculated lifetimes are summarized in Table 1. The granulated particles ( $S_2$ ) prepared without the use of TEOT has an electron lifetime of 6.3 ms, which is smaller than that (8.6 ms) of the electrode  $S_1$  fabricated by using nanoparticles themselves. On the contrary, the electron lifetime (11.7 ms) of TEOT-modified granules ( $S_3$ ) is larger than those of other two electrodes. When compared to the nano-sized  $\text{TiO}_2$ , the relatively low light-harvesting efficiency of the granular  $\text{TiO}_2$  prepared without adding TEOT is attributed to the large transport resistance as well as the short lifetimes of electrons. The increase in the electron lifetimes means the increase in the diffusion length of photo-excited electron as well as the decrease in the charge recombination reaction of photo-excited electrons with  $\text{I}_3^-$  within photoanodes. As a result, more effective light-harvesting efficiency could be achieved by using the  $\text{TiO}_2$  granules having the chemical interconnection of nanoparticles. From the results so far, we have confirmed that the addition of TEOT to the spray colloidal solution could form a chemical connection between nanoparticles and be helpful for preparing mesoporous granular particles having an improved light-harvesting efficiency of dye-sensitized solar cells.

#### 4. Conclusions

This work suggests a simple and effective way to improve the light-harvesting efficiency of mesoporous  $\text{TiO}_2$  granules prepared by spray pyrolysis process using a colloidal precursor solution. The chemical interconnection of nanoparticles within the granules was generated by adding TEOT to the spray solution to improve the light-harvesting efficiency of DSSCs. The prepared granules had pure anatase phase, with an average particle size of about 400 nm. The TEOT-modified  $\text{TiO}_2$  granules enhanced light scattering, compared with the nano-sized  $\text{TiO}_2$  in the photoelectrode. The chemical interconnection of nanoparticles within granules, which was successfully achieved

by adding TEOT to the colloidal spray solution, led to effectively reducing the resistance at the  $\text{TiO}_2$ /dye/electrolyte interface as well as increasing the lifetimes of photo-excited electrons. Thus, the solar conversion efficiency of the  $\text{TiO}_2$  granules was improved about 20% compared with the granules without the chemical connection, and 14% higher than the nanoparticles.

#### Acknowledgments

This work was supported by a research grant of Kongju National University in 2013.

#### References

- O'Regan, B. and Grätzel, M., "A Low-cost, High-efficiency Solar Cell Based on Dye-sensitized Colloidal  $\text{TiO}_2$  Films," *Nature*, **353**, 737-740(1991).
- Rhee, S.-W. and Kwon, W., "Key Technological Elements in Dye-sensitized Solar Cell," *Korean J. Chem. Eng.*, **28**(7), 1481-1494 (2011).
- Wang, Z.-S., Kawauchi, H., Kashima, T. and Arakawa H., "Significant Influence of  $\text{TiO}_2$  Photoelectrode Morphology on the Energy Conversion Efficiency of N719 Dye-sensitized Solar Cell," *Coordination Chem. Rev.*, **248**, 1381-1389(2004).
- Park, N.-G., "Light Management in Dye-sensitized Solar Cell," *Korean J. Chem. Eng.*, **27**(2), 375-384(2010).
- Jang, K.-I., Hong, E. and Kim, J. H., "Effect of An Electrodeposited  $\text{TiO}_2$  Blocking Layer on Efficiency Improvement of Dye-sensitized Solar Cell," *Korean J. Chem. Eng.*, **29**(3), 356-361 (2012).
- Battumur, T., Yang, W., Ambade, S. B. and Lee, S.-H., "Dye-sensitized Solar Cell Based on  $\text{TiO}_2$ -graphene Composite Electrodes," *Korean Chem. Eng. Res.*, **50**(1), 177-181(2012).
- Kim, H.-N. and Moon, J. H., "Enhanced Photovoltaic Properties of  $\text{Nb}_2\text{O}_5$ -coated  $\text{TiO}_2$  3D Ordered Porous Electrodes in Dye-sensitized Solar Cells," *Appl. Mater. Interf.*, **4**(11), 5821-5825(2012).
- Zuh, X., Tsuji, H., Yella, A., Chauvin, A.-S., Grätzel, M. and Nakamura, E., "New Sensitizers for Dye-sensitized Solar Cells Featuring a Carbon-bridged Phenylenevinylene," *Chem. Commun.*, **49**, 582-584(2013).
- Lee, S., Jeon, Y., Lim, Y., Hossain, Md. A., Lee, S., Cho, Y., Ju, H. and Kim, W., "A New Siloxane Containing Imidazolium Iodide as Electrolyte for Dye-sensitized Solar Cell," *Electrochim. Acta*, **107**, 675-680(2013).
- Ludin, N. A., Mahmoud, A. M. A.-A., Mohamad, A. B., Kadhum, A. A. H., Sopian, K. and Karim, N. S. A., "Review on the Development of Natural Dye Photosensitizer for Dye-sensitized Solar Cells," *Renew. Sust. Energ. Rev.*, **31**, 386-396(2014).
- Sabba, D., Agarwala, S., Pramana, S. S. and Mhaisalkar S., "A Maskless Synthesis of  $\text{TiO}_2$ -nanofiber-based Hierarchical Structures for Solid-state Dye-sensitized Solar Cells with Improved Performance," *Nanoscale Res. Lett.*, **9**, 14-22(2014).
- Lamberti, A., Sacco, A., Bianco, S., Manfredi, D., Cappelluti, F., Hernadez, S., Quaglio, M. and Pirri C. F., "Charge Transport Improvement Employing  $\text{TiO}_2$  Nanotube Arrays as Front-side Illuminated Dye-sensitized Solar Cell Photoanodes," *Phys. Chem. Chem. Phys.*, **15**, 2596-2062(2013).

13. Sauvage, F., Chen, D., Comte, P., Huang, F., Heiniger, L.-P., Cheng, Y.-B., Caruso, R. A. and Graetzel, M., "Dye-sensitized Solar Cells Employing a Single Film of Mesoporous TiO<sub>2</sub> Beads Achieve Power Conversion Efficiencies over 10%," *ACS Nano*, **4**(8), 4420-4425 (2010).
14. Lee, S.-W., Ahn, K.-S., Zhu, K., Neale, N. R. and Frank, A. J., "Effect of TiCl<sub>4</sub> Treatment of Nanoporous TiO<sub>2</sub> Films on Morphology, Light Harvesting, and Charge-carrier Dynamics in Dye-sensitized Solar Cells," *J. Phys. Chem. C*, **116**, 21285-21290(2012).
15. O'Regan, B. C., Durrant, J. R., Sommeling, P. M. and Bakker, N. J., "Influence of the TiCl<sub>4</sub> Treatment on Nanocrystalline TiO<sub>2</sub> Films in Dye-sensitized Solar Cells. 2. Charge Density, Band Edge Shift, and Quantification of Recombination Losses at Short Circuit," *J. Phys. Chem. C*, **111**, 14001-14010(2007).
16. Fuke, N., Katoh, R., Islam, A., Kasuya, M., Furube, A., Fukui, A., Chiba, Y., Komiya, R., Yamanaka, R., Han, L. and Harima H., "Influence of TiCl<sub>4</sub> Treatment on Back Contact Dye-sensitized Solar Cells Sensitized with Black Dye," *Energ. Environ. Sci.*, **2**, 1205-1209(2009).
17. Chen, D., Huang, F., Cheng, Y.-B. and Caruso, R. A., "Mesoporous Anatase TiO<sub>2</sub> Beads with High Surface Area and Controllable Pore Sizes: A Superior Candidate for High-performance Dye-sensitized Solar Cell," *Adv. Mater.*, **21**, 2206-2210(2009).
18. Wang, Q., Moser, J.-E. and Grätzel, M., "Electrochemical Impedance Spectroscopic Analysis of Dye-sensitized Solar Cell," *J. Phys. Chem. B*, **109**(31), 14945-14953(2005).
19. Bisquert, J., Fabregat-Santiago, F., Mora-Seró, I., Garcia-Belmonte, G. and Giménez S., "Electron Lifetime in Dye-sensitized Solar Cell: Theory and Interpretation of Measurements," *J. Phys. Chem. C*, **113**(40), 17278-17290(2009).